

Adiabatic shear banding in a thick-walled steel tube

R. C. Batra, D. Rattazzi

412

Abstract We analyze the initiation and propagation of adiabatic shear bands in a thick-walled 4340 steel tube with a V-notch in the middle. The material is modeled as strain hardening, strain-rate hardening and thermal softening. The deformations are assumed to be locally adiabatic and the effect of inertia forces is considered. Two different loadings, i.e., torsional, and combined torsional and axial pressure are considered. In each case, the load generally increases linearly from zero to the final value, is kept steady there for some time, then decreases to zero and is kept at zero; thus a finite amount of energy is input into the body. For the combined loading, the magnitude of the torsional loading pulse is kept fixed and the effect of varying the magnitude of the axial pressure preload is investigated. A shear band first initiates in the element adjoining the notch tip and propagates radially inwards. By recording the time when a shear band initiates at the centroids of different elements we determine its speed of propagation in the radial direction to vary from approximately 50 m/s at the instant of its initiation in an element abutting the notch tip, to nearly 90 m/s by the time it reaches the innermost surface of the tube; the speed also depends upon the overall loading rate, and whether or not the loading is multiaxial. The drop in the torque required to twist the tube at the initiation of a shear band is not as sharp as that in a thin-walled steel tube. We compute the distance through which a shear band propagates as a function of the energy input into the body and thus ascertain the energy required to drive a shear band through a unit distance.

We also study torsional deformations of a thick-walled CR-300 steel tube, model its thermal softening by a relation proposed by Zhou et al. and use material properties derived from their data. In this case, the speed of a shear

band initiating from an element abutting the notch tip is found to vary between 750 m/s and 1,000 m/s at different points on a radial line through the notch tip; this agrees with that observed by Zhou et al. in their experiments on single-notched plates.

1 Introduction

Since shear bands usually precede shear fractures in impulsively loaded ductile materials, their study has drawn considerable attention. Even though Tresca (1878) observed them over a century ago during the hot forging of a platinum bar, the activity in the field has picked up since 1944 when Zener and Hollomon (1944) reported observing shear bands during the punching of a hole in a low carbon steel plate. A shear band is a narrow region, usually a few microns (micrometers) wide, that forms in high strain-rate deformations of many metals and some polymers. The primary mode of deformation in these narrow regions is simple shearing. They are called adiabatic since they fully develop in a few microseconds and there is not enough time for the heat to be conducted out of these severely deformed regions. Zener and Hollomon (1944) postulated that the material becomes unstable when the softening caused by heating due to plastic deformation equals the hardening of the material due to strain and strain-rate effects. Analytical works (e.g. see Clifton 1980; Anand et al. 1987) have assumed that a shear band initiates when the shear stress in a simple shearing problem or the effective stress in a three dimensional problem attains its maximum value. Much of the work done during the last two decades is reviewed in papers included in works edited by Zbib et al. (1992), Armstrong et al. (1994) and Batra and Zbib (1994). Two of the unresolved issues are the energy required to drive a shear band and the effect of a multiaxial state of stress on the initiation and propagation of an adiabatic shear band. We attempt to address these issues by studying the initiation and propagation of an adiabatic shear band in an impulsively loaded thick-walled steel tube with a V-notch at the midsection. The stress state near the notch root is expected to be triaxial and because of the stress concentration, a shear band should initiate there first. Previous experimental (e.g. see Marchand and Duffy 1988) works on the torsion of thin-walled steel tubes and their numerical simulation (Wright and Walter 1987; Batra and Kim 1992) as simple shearing problems have revealed that the shear stress drops catastrophically at the instant of the initiation of a shear band. Batra and Zhang (1994) studied numerically the torsion of a thin-walled steel tube

Communicated by S. N. Atluri, 25 February 1997

R. C. Batra, D. Rattazzi
Department of Engineering Science and Mechanics,
Virginia Polytechnic Institute and State University,
Blacksburg, VA 24061-0219, USA

Correspondence to: R. C. Batra

This work was supported by the Army Research Office grant DAAH04-95-1-0043, ONR grant N00014-94-1-1211, and the National Science Foundation grant CMS9411383 to Virginia Polytechnic Institute and State University.

as a 3-dimensional problem and assumed that the yield stress of a small region near the center of the tube was 5% less than that of the rest of the material. They found that the torque required to deform the tube dropped very rapidly when a shear band, as evidenced by distortions of the deformed mesh, initiated.

2 Formulation of the problem

We use the referential or Lagrangian description of motion to study dynamic thermomechanical deformations of a thick-walled steel tube; these deformations are governed by the following balance laws of mass, linear momentum, moment of momentum and internal energy (e.g. see Truesdell and Noll 1965).

$$\rho J = \rho_0 \quad (1)$$

$$\rho_0 \dot{\mathbf{v}} = \text{Div } \mathbf{T} \quad (2)$$

$$\mathbf{F}^T \mathbf{T} = \mathbf{T}^T \mathbf{F} \quad (3)$$

$$\rho_0 \dot{e} = \text{tr}(\mathbf{T} \dot{\mathbf{F}}^T) \quad (4)$$

Here ρ_0 is the mass density of a material particle in the reference configuration, ρ its present mass density, \mathbf{F} the deformation gradient, $J = \det \mathbf{F}$, \mathbf{v} the present velocity of a material particle, a superimposed dot denotes the material time derivative, \mathbf{T} the first Piola-Kirchhoff stress tensor, \mathbf{F}^T the transpose of \mathbf{F} , e the internal energy density, tr denotes the trace operator and Div signifies divergence with respect to coordinates in the reference configuration. In Eq. (4) the effect of heat conduction has been neglected. This is justified because a shear band develops in a few microseconds and there is not enough time for the heat to be conducted out of the band. Batra and Kim (1991) have shown through numerical experiments that heat conduction has a negligible effect on the time of initiation of a shear band. As is the case in continuum mechanics, we require that the balance of moment of momentum (3) be identically satisfied. In Eq. (4) we have assumed that all of the plastic working, rather than 90–95% of it as asserted by Farren and Taylor (1925) and Suljoadikusumo and Dillon (1979), is converted into heating. We postulate the following constitutive relations for the material of the tube.

$$\mathbf{T} = J \boldsymbol{\sigma} (\mathbf{F}^{-1})^T, \quad \boldsymbol{\sigma} = -p \mathbf{1} + \mathbf{S}, \quad p = K(\rho/\rho_0 - 1), \quad (5)$$

$$\overset{\nabla}{\mathbf{S}} = 2\mu(\overline{\mathbf{D}} - \overline{\mathbf{D}}^p), \quad \overset{\nabla}{\mathbf{S}} = \dot{\mathbf{S}} + \mathbf{S}\mathbf{W} - \mathbf{W}\mathbf{S}, \quad (6)$$

$$\mathbf{D} = \frac{1}{2}(\text{grad } \mathbf{v} + (\text{grad } \mathbf{v})^T), \quad (7)$$

$$\mathbf{W} = \frac{1}{2}(\text{grad } \mathbf{v} - (\text{grad } \mathbf{v})^T), \quad (7)$$

$$\overline{\mathbf{D}} = \mathbf{D} - \frac{1}{3}(\text{tr} \mathbf{D}) \mathbf{1}, \quad (8)$$

$$\text{tr } \mathbf{D}^p = 0, \quad \mathbf{D}^p = \Lambda \mathbf{S}, \quad S_e^2 \equiv \frac{3}{2} \text{tr}(\mathbf{S}\mathbf{S}^T) = \sigma_y^2, \quad (8)$$

$$\dot{e} = c\dot{\theta} + \text{tr}(\boldsymbol{\sigma} \mathbf{D}^e), \quad (9)$$

$$\sigma_y = (A + B(\epsilon^p)^n)(1 + C \ln(\dot{\epsilon}^p/\dot{\epsilon}_0))(1 - T^m), \quad (9)$$

$$T = (\theta - \theta_0)/(\theta_m - \theta_0), \quad (\dot{\epsilon}^p)^2 = \frac{2}{3} \text{tr}(\mathbf{D}^p \mathbf{D}^p). \quad (10)$$

Here $\boldsymbol{\sigma}$ is the Cauchy stress tensor, \mathbf{S} its deviatoric part, p the hydrostatic pressure taken to be positive in compression, K the bulk modulus, μ the shear modulus, $\overset{\nabla}{\mathbf{S}}$ the Jaumann derivative of \mathbf{S} , $\overline{\mathbf{D}}$ the deviatoric strain-rate, \mathbf{D}^p the plastic strain-rate, \mathbf{D}^e the elastic strain-rate, $\mathbf{D} = \mathbf{D}^e + \mathbf{D}^p$ the strain-rate tensor, \mathbf{W} the spin tensor, c the specific heat, θ the temperature of a material particle, θ_m its melting temperature, θ_0 the room temperature, T the homologous temperature, S_e the effective stress, and ϵ^p the effective plastic strain. Equation (5)₃ implies that the volumetric response of the material is elastic. Equation (6)₁ is the constitutive relation in terms of deviatoric stresses for a linear isotropic hypoelastic material, $\text{grad } \mathbf{v}$ equals the gradient of the velocity field with respect to coordinates in the present configuration, Eq. (8)₄ signifies the von Mises yield criterion with isotropic hardening, and Eq. (9)₂ is the Johnson-Cook (1983) relation. The flow stress, σ_y , increases with an increase in the effective plastic strain and the effective plastic strain rate but decreases with an increase in the temperature of a material particle. Truesdell and Noll (1965) have pointed out that Eq. (6)₁ is not invariant with respect to the choice of different objective (or material frame indifferent) time derivatives of the stress tensor. In Eq. (9)₂ parameters B and n characterize the strain hardening of the material, C and $\dot{\epsilon}_0$ its strain-rate hardening and $(1 - T^m)$ its thermal softening. Equation (8)₃ signifies that the plastic strain-rate is along the normal to the yield surface (8)₄, and the factor of proportionality Λ is given by

$$\Lambda = 0 \text{ when either } S_e < \sigma_y, \text{ or } S_e = \sigma_y \text{ and } \text{tr}(\mathbf{S}\mathbf{D}^p) < 0; \quad (11)$$

otherwise it is a solution of

$$S_e = (A + B(\epsilon^p)^n)(1 + C \ln(\frac{2}{3} \Lambda S_e / \dot{\epsilon}_0))(1 - T^m). \quad (12)$$

Our constitutive hypotheses (5) and (9)₂ imply that the flow stress required to plastically deform a material point vanishes once its temperature equals the melting temperature of the material; the material point will then behave as a compressible, nonviscous fluid. In physical experiments, fracture in the form of a crack will ensue from the point much before it is heated up to the melting temperature. Here we have not incorporated any fracture criterion into the problem formulation, and in our numerical simulations for the 4340 steel tube, no material point reaches its melting temperature.

We take the body to be initially at rest, stress free and at a uniform temperature θ_0 . All bounding surfaces of the tube are taken to be thermally insulated; this is consistent with the assumption of locally adiabatic deformations. One end face of the tube is rigidly clamped and the other end is loaded either by a prescribed angular speed, or a normal pressure followed by a prescribed angular speed. In each case, the prescribed variable increases linearly in time from zero to the assigned value in 20 μs , stays there for the desired duration, and then decreases linearly to zero in 20 μs . The time duration during which the prescribed quantity stays fixed is varied to change the energy input into the system. The rise time of 20 μs is typical of torsional tests conducted in a split Hopkinson bar.

3

Computation and discussion of results

We assigned the following values to various material and geometric parameters in order to compute numerical results presented and discussed below in Sects. 3.1 through 3.3.

$$\rho_0 = 7,840 \text{ kg/m}^3, \quad \mu = 76 \text{ GPa}, \quad K = 157 \text{ GPa}$$

$$A = 792.2 \text{ MPa}, \quad B = 509.5 \text{ MPa}, \quad n = 0.26,$$

$$C = 0.014, \quad m = 1.03$$

$$\theta_m = 1793 \text{ K}, \quad \theta_0 = 298 \text{ K}, \quad \dot{\epsilon}_0 = 1/s, \quad c = 477 \text{ J/kg}^\circ\text{C}$$

$$\text{Inner radius} = 1.27 \text{ mm}, \quad \text{Outer radius} = 4.445 \text{ mm},$$

$$\text{Tube length} = 16.51 \text{ mm} . \quad (13)$$

The values of material parameters in the Johnson-Cook model for the 4340 steel are taken from Rajendran (1992). The range of effective plastic strains, effective plastic strain rates and temperatures used to obtain these values is much smaller than that likely to occur in a shear band problem. Klepaczko et al. (1987) have pointed out that nearly all of the material parameters in (13) depend upon the temperature. However, such temperature dependence is not considered herein primarily because of the difficulty in finding test data over the wide range of strains, strain-rates and temperatures likely to occur within a shear band.

The coupled thermomechanical problem formulated in the preceding section is highly nonlinear and cannot be solved analytically; therefore we seek its approximate solution by the finite element method and employ the large scale explicit finite element code DYNA3D developed by Whirley and Hallquist (1991). The code uses 8-noded brick elements, one-point quadrature rule, an hour-glass control to suppress spurious modes, and adjusts the time step adaptively to satisfy the Courant condition; thus the stability condition is satisfied. Because of the use of a one-point integration rule, stresses, strains and temperatures in an element are assumed to be constants. In DYNA3D, artificial bulk viscosity is added to smear out the shocks; this may influence the time at which a shear band initiates. In this method, the pressure in elements being compressed is augmented by an artificial viscous term q given by

$$q = \rho \hat{l} |\text{tr}(\mathbf{D})| (Q_1 \hat{l} |\text{tr}(\mathbf{D})| + Q_2 \hat{c}) . \quad (14)$$

Here Q_1 and Q_2 are dimensionless constants which default to 1.5 and 0.06 respectively, \hat{l} is the cube root of the volume of the element, \hat{c} is the speed of sound in the material and equals $((K + 4\mu/3)/\rho_0)^{1/2}$. Batra and Adulla (1995) have shown that different values of Q_1 and Q_2 have virtually no effect on the instant of initiation of an adiabatic shear band. Results presented below are for default values of Q_1 and Q_2 . The code neglects the effect of heat conduction which has the advantage that the time step, Δt , is controlled by the mechanical problem, and the temperature rise, $\Delta\theta$, at the centroid of an element is computed from

$$\rho c \Delta\theta = \text{tr}(\mathbf{SD}^p) \Delta t \quad (15)$$

which follows from Eqs. (4), (5), (8)_{1,2} and (9)₁.

The finite element mesh generally consisted of 11 elements in the radial direction, 71 elements in the axial di-

rection and 108 elements in the circumferential direction; a finer mesh could not be used within available computational resources. The mesh was essentially uniform in the radial direction but was slightly graded in the axial direction away from the notch; the aspect ratio for elements near the notch was close to 1, while the remainder of the elements had aspect ratios no greater than 3.5. As shown by Batra and Ko (1992), an adaptively refined mesh gives sharper results for the rate of evolution of a quantity within a shear band but does not affect when a shear band initiates. Since most of the results presented herein involve the initiation of a shear band, they are representative of the problem studied. For comparison purposes, we analyse torsional deformations of the same steel tube but only 3 mm in length with 28 uniform elements in the radial direction, 17 elements in the axial direction and 250 elements in the circumferential direction. Because of our desire to directly evaluate quantities at points on the midsurface of the tube, the mesh had one row of elements with their centroids at the midsurface. This blunted the root of the V -notch causing the notch to look more like an open channel; a finite element discretization of the tube and a sketch of the V -notch are shown in Fig. 1. The notch shape was varied by changing the dimension d ; it equals 0.142, 0.221, 0.3, 0.379 and 0.458 mm respectively, for notches 1, 2, 3, 4 and 5.

3.1

Torsion of the tube

The tube is deformed by keeping one end face stationary and twisting the other end face by prescribing on it an angular speed that increases linearly from zero to the maximum value, ω_0 , in 20 μs , keeping it steady for t_r microseconds, then decreasing it linearly to zero in 20 μs and keeping it at zero. The average shear strain-rate is least for points on the inner surface of the tube and most at points on the outer surface. As should be clear from the distribution of the effective plastic strain on a radial line plotted in Fig. 2 for different values of the maximum angular

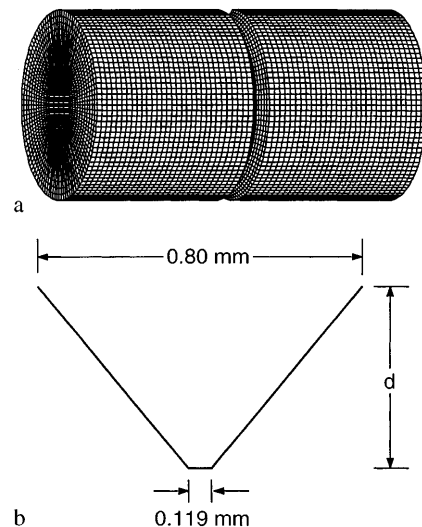


Fig. 1. a Finite element discretization of the tube, and b Details of the notch

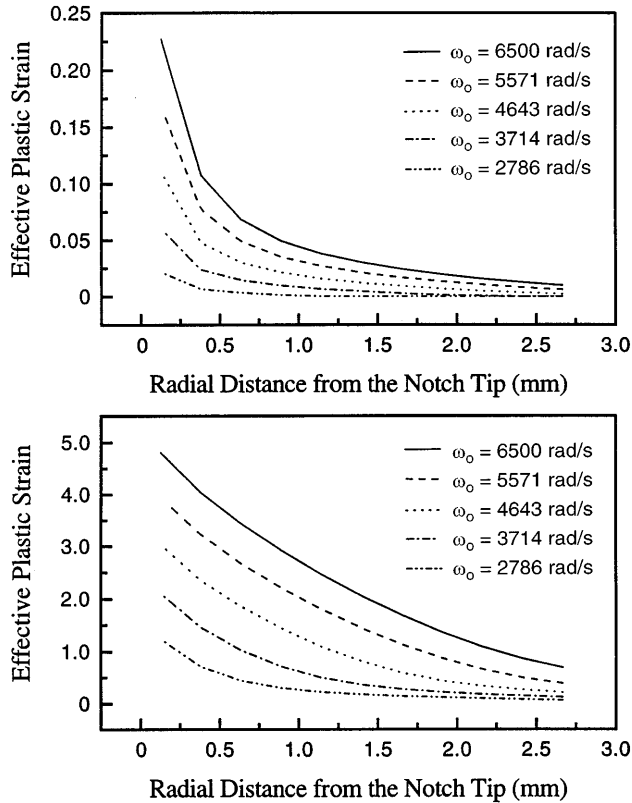


Fig. 2a,b. Distribution of the effective plastic strain on a radial line for notch 4 with different values of the maximum applied angular speed; a $t = 20 \mu\text{s}$, b $t = 70 \mu\text{s}$

speed applied to notch 4, and for a $70 \mu\text{s}$ total duration of the loading pulse, at lower values of the prescribed maximum angular speed elements below the notch tip do not undergo much plastic deformation at $t = 20 \mu\text{s}$. Even at $t = 70 \mu\text{s}$ and $\omega_0 = 2786 \text{ rad/s}$ the material in nearly half of the thickness of the tube adjoining its inner surface has an effective plastic strain of at most 0.25. This is because the external work done during the loading of the body or the energy supplied by the loading pulse is not enough to cause intense plastic deformations of the material underneath the notch bottom. Figure 3 depicts the time history of the effective stress, effective plastic strain and temperature at the centroids of 11 elements on a radial line through the notch tip for $\omega_0 = 6500 \text{ rad/s}$ and $t_r = 30 \mu\text{s}$; curve 1 is for the first element below the notch tip, and curve 11 is for the element adjoining the inner surface of the tube. Even though the problem was analyzed as three-dimensional, the deformations were found to be independent of the angular position of a material point. It is clear from these plots that once the elastic shear loading wave arrives at the centroid of the notch at about $2.65 \mu\text{s}$, the effective stress in the element abutting the notch root rises sharply because of the stress concentration there. We note that the elastic shear loading wave arrives at these eleven elements at the same time. The different rate of rise of the effective stress in these elements is due to the fact that the average shear strain-rate and thus the average shear strain increases, at least during the initial elastic part of deformations, with the radial distance of a point from

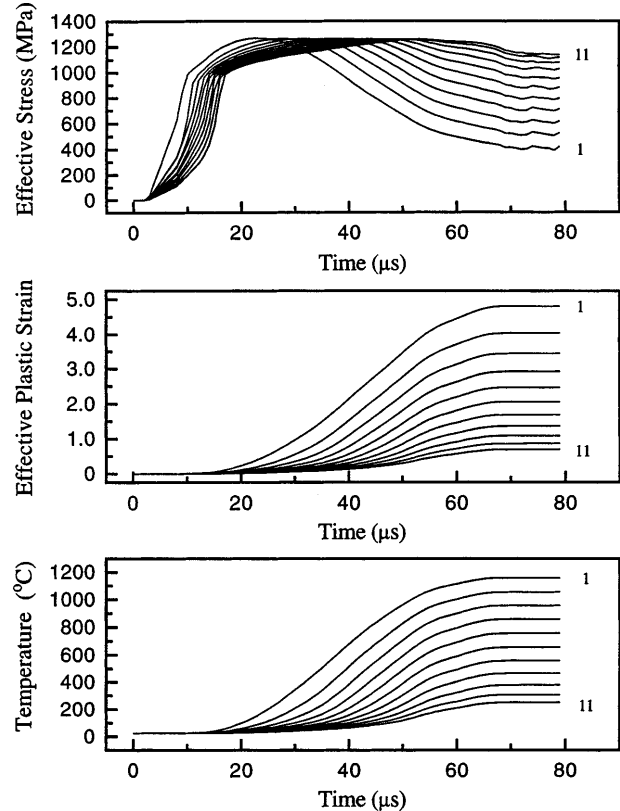


Fig. 3a-c. Time history of a the effective stress, b the effective plastic strain, and c the temperature at the centroids of eleven elements on a radial line through the notch tip, for notch 4 with $\omega_0 = 6500 \text{ rad/s}$

the tube's axis. Also, the effects of stress concentration and the triaxiality of deformations due to the notch diminish rapidly with the distance from the notch tip; we address these issues a little later. Since the effective stress after having reached its peak value drops rather gradually, it is hard to decide when a shear band initiates. We note that during torsional tests on thin-walled tubes, Marchand and Duffy (1988) observed a catastrophic drop in the shear stress at the initiation of a shear band; similar rapid drops in the shear stress were computed by Wright and Walter (1987) during their numerical simulations of the test as a simple shearing problem, and by Batra and Zhang (1994) who analyzed it as a three-dimensional problem. Batra and Kim (1992) studied the simple shearing problem for twelve materials and postulated that a shear band initiates in earnest when the shear stress has dropped to 90% of the peak value. Deltort (1994) has associated the initiation of severe localization of deformation with the instant when the shear stress has dropped to 80% of its peak value. Analytical works (e.g. see Clifton 1980) usually assume that a shear band initiates when the shear stress in a simple shearing problem attains its peak value. Marchand and Duffy did not report the values of the effective plastic strain within a shear band at the instant of its initiation, but indicated a maximum shear strain of 20 within a fully developed band. Zhou et al. (1996) studied the development of shear bands in a single-notched CR-300 steel plate and assumed that a material particle within a shear band fails and subsequently behaves as a nonlinear viscous fluid

once the effective plastic strain there equals 0.4. As is evident from the plots of the evolution of the effective plastic strain and the temperature, their values at the instant of initiation of a shear band will vary with the criterion used for the initiation of a shear band. For example, at the instant of the effective stress attaining its peak value in the element just below the notch tip, the effective plastic strain and the temperature in it equal 0.39 and 154°C respectively. However, when the effective stress has dropped to 90% of its peak value in that element, the effective plastic strain and the temperature there equal 1.26 and 436°C respectively. In either case, the temperature in the element at the instant a shear band initiates is nowhere close to its melting temperature. Of course, the temperature and the effective plastic strain there continue to increase at an increasing rate during the postlocalization period until the time the loaded end is brought to rest and is subsequently kept at rest. The temperature in the element below the notch tip at $t = 60 \mu\text{s}$ reaches 1156°C, which equals 80% of the presumed melting temperature of the material.

By adopting a criterion for the initiation of a shear band, one can ascertain the time at which a shear band initiates in different elements on a radial line through the notch tip and thus compute the band speed in the radial direction. Figure 4 shows the dependence of the time of initiation of a shear band in the first element below the notch tip on the prescribed angular speed as computed by the following three criteria: (i) the effective plastic strain equals 0.50, (ii) the effective stress attains its maximum value, and (iii) the effective stress has dropped to 90% of its maximum value. It is clear from the figure that the initiation time depends on the rate of loading as well as the definition chosen to characterize the initiation of a shear band. Figure 5 illustrates, for $\omega_0 = 6500 \text{ rad/s}$, the variation of the band speed with the radial distance from the notch tip computed by criterion (ii) and (iii) stated above, and by the following additional criteria: (iv) the effective plastic strain equals 0.46, and (v) the effective plastic strain equals 0.90. For each case, the band speed starts out at

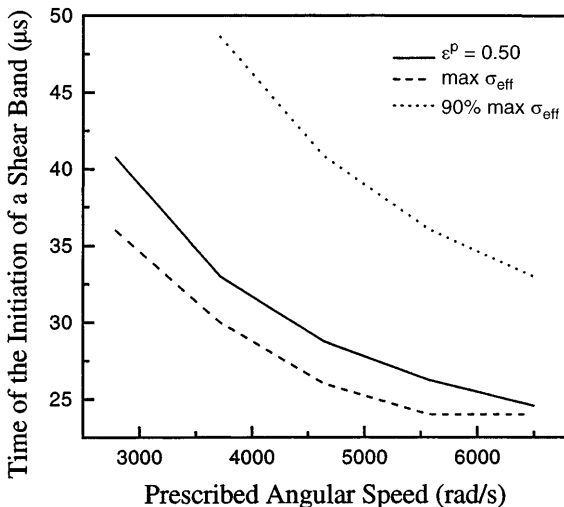


Fig. 4. Dependence of the time of initiation of a shear band on the prescribed angular speed, calculated by three different criteria, for notch 4 and a load duration of 70 μs

about 50 m/s when it initiates in an element just below the notch root, and begins to increase as it propagates radially inwards; the variation of speed with the radial distance is not monotonic. Both the band speed and its variation with the radial distance depend strongly upon the criterion used for the initiation of a shear band; the maximum computed band speed is 130 m/s. Possible reasons for getting an erratic variation of the band speed with the radial distance obtained by using criterion (ii) are the coarseness of the finite element mesh, the discrete times at which the output is printed, and the error in estimating exactly when the peak stress occurs in an element. Peng and Batra (1995) analyzed shear bands in a 4340 steel thick-walled tube with a hemispherical cavity centered at the outer surface of the midsection of the tube. In this case a shear band initiating at the bottom of the cavity could propagate in the axial, circumferential, and radial direc-

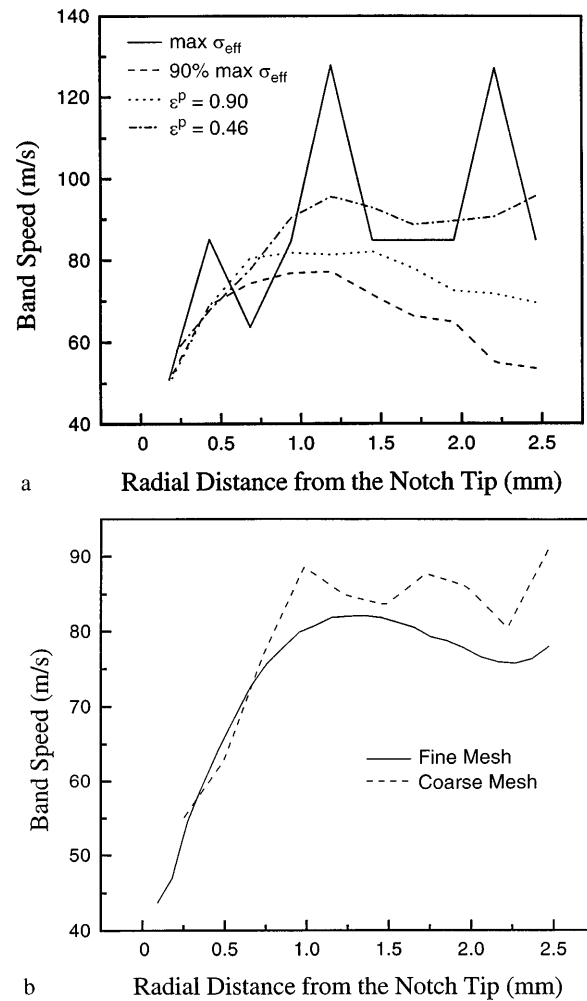


Fig. 5a,b. a Band speed according to different initiation criteria vs. the radial distance from the notch tip; the band initiates when the effective stress attains its maximum value, the effective stress has dropped to 90% of its maximum value; and the effective plastic strain equals 0.46 and 0.90 respectively. Results are for notch 4 with $\omega_0 = 6500 \text{ rad/s}$. b Effect of mesh size on the band speed vs. the radial distance through which a shear band (a contour of effective plastic strain of 0.50) has propagated. Results are for notch 5 with $\omega_0 = 6500 \text{ rad/s}$

tions. They found that a contour of effective plastic strain of 0.7 propagated in the circumferential and radial directions at approximately 600 m/s and 60 m/s respectively, and the speed increased in both directions as the band propagated further. We note that the band speed in the circumferential direction is influenced by the tangential velocity of material particles. Marchand and Duffy (1988) reported that a shear band initiating from a point defect in a thin-walled HY-100 steel tube propagated in the circumferential direction either at an average speed of 520 m/s or at 260 m/s depending upon whether it traveled in one direction only, or in both directions at the same speed. Computational work of Batra and Zhang (1994) supports the second alternative suggesting that the average shear band speed in Marchand and Duffy's work was 260 m/s.

In an attempt to delineate the effect of the mesh on the computed band speeds, we analysed torsional deformations of the same steel tube but only 3 mm long. The region was divided into 28 uniform elements in the radial direction, 17 elements in the axial direction and 250 elements in the circumferential direction. As illustrated in Fig. 5b, the speeds of contour of $\epsilon^p = 0.5$ computed with the two meshes agree with each other. After the band has propagated radially inwards through 1 mm, the band speed equals nearly 80 m/s.

As can be inferred from the plots of Fig. 3, at the instant of the initiation of a shear band in the element just below the notch tip, according to any one of the aforementioned criteria, there is a steep gradient in the distribution of the temperature and the effective plastic strain on a radial line through the notch tip. Even when the shear band has propagated to the innermost surface of the tube, the temperature and the plastic strain vary through the thickness of the tube. At a material point, these quantities vary with time even when the band speed is nearly uniform. In the spatial description, a steady state is reached only when $t \geq 70 \mu\text{s}$ since the two end faces of the tube are subsequently kept fixed. The consideration of heat conduction would tend to stabilize these fields sooner.

In Fig. 6 we have plotted the time history of the torque required to deform the tube with notch 4 for three different durations of the applied angular speed; in each case the angular speed increases linearly from zero to the steady value of 6500 rad/s in 20 μs and eventually decreases linearly to zero in 20 μs . There is no sharp drop in the torque, as in the case of a thin-walled tube, to signify the initiation of a shear band. In a thin-walled tube a shear band essentially initiates simultaneously at all points on a radial line through the point of minimum wall thickness. Once it happens, the load carrying capacity of the tube is significantly diminished. For a thick-walled tube even when a shear band initiates in an element on the outer surface of the tube, elements interior to it are either deforming elastically or even if deforming plastically may still be on the rising part of the effective stress vs. effective strain curve. Thus the torque required to deform the tube may even increase first and then decrease gradually. The maximum value of the torque occurs at about $t = 20 \mu\text{s}$ when the prescribed angular speed attains its steady value. For this loading condition, at $t = 20 \mu\text{s}$, elements just be-

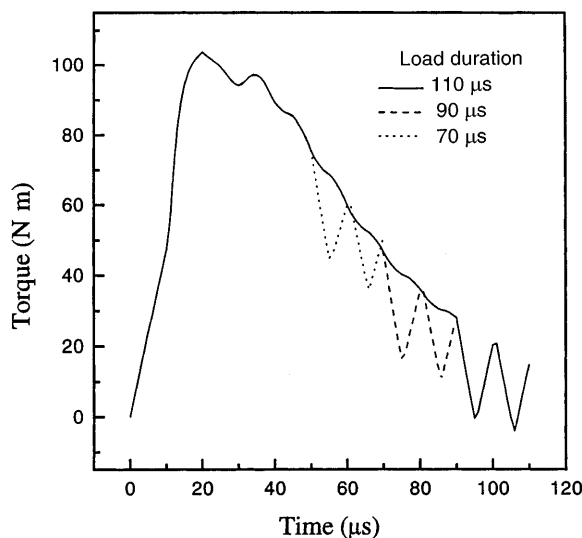


Fig. 6. Time history of the torque required to deform the tube with notch 4 for three different durations of the applied angular speed, with $\omega_0 = 6500 \text{ rad/s}$

low the notch tip have started to soften in the sense that the effective stress there has peaked and has started to decrease. When the prescribed angular speed begins to decrease, the torque drops quickly to indicate the onset of an elastic unloading wave. The time period of the oscillations in the torque equals the time taken for an elastic wave to propagate through twice the length of the tube.

Figure 7 depicts the deformed configuration, at $t = 100 \mu\text{s}$, of a plane passing through the tube's axis when the total load duration equals 110 μs . It is clear that only the material layer beneath the notch tip undergoes severe plastic deformations; it was confirmed by plotting the distribution of the effective plastic strain on an axial line. The plot, not shown here for the sake of brevity, indicated that for $t \geq 30 \mu\text{s}$, the plastic strain accumulated only within this one element thick layer below the notch bottom. The band width, defined as the thickness in the axial direction of the severely deformed region, equals the axial dimension of the element abutting the bottom surface of the notch. Of course, one needs a much finer mesh to estimate the width of a shear band. As mentioned earlier, the available computational resources limited the fineness of the mesh. The time history of the kinetic energy of the material to the left and right of the one-element wide shear band, plotted in Fig. 8 for notch 5 with $\omega_0 = 6500 \text{ rad/s}$, indicates that subsequent to the initiation of a shear band at $t \approx 20 \mu\text{s}$, the material to its right is virtually stationary and that to its left moves as a rigid body. Thus the tan-

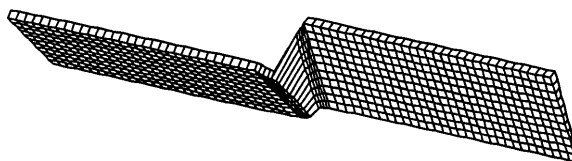


Fig. 7. Deformed configuration of a plane passing through the tube's axis at $t = 100 \mu\text{s}$ for notch 4 with $\omega_0 = 6500 \text{ rad/s}$ and a load duration of 110 μs

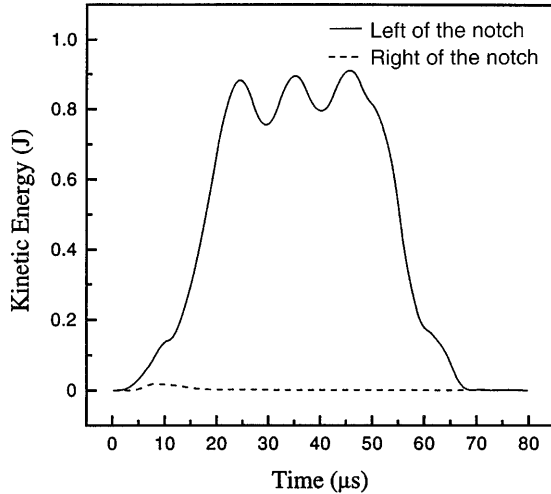


Fig. 8. Time history of the kinetic energy of the material to the left and right of the notch for notch 5 with $\omega_0 = 6500$ rad/s

gential velocity is discontinuous across a shear band; a similar conclusion was drawn by Batra and Jin (1994) who studied the development of a shear band in a porous elasto-thermo-viscoplastic material deformed in plane strain tension and confirms Tresca's (1878) conjecture.

From the time history of the torque plotted in Fig. 6 and knowing the prescribed angular speed, we can compute the work done by external forces or energy input into the body. A part of this energy is used to change the kinetic energy of the body and the rest to deform it. The strain energy density of the elastic deformations is negligible as compared to the work done/volume required to plastically deform the body. After a shear band has initiated in elements below the notch tip, the kinetic energy of the tube remains essentially uniform until the prescribed angular speed begins to decrease. We have plotted in Fig. 9 the work done by external force versus the radial distance through which a shear band, defined as a contour of effective plastic strain of 0.5, has propagated for notch 4 with $\omega_0 = 6500$ rad/s; the plot is essentially a straight line.

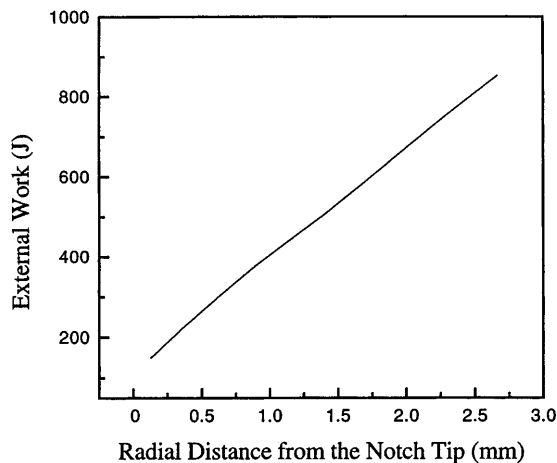


Fig. 9. External work done vs. the radial distance through which a shear band (a contour of effective plastic strain of 0.50) has propagated for notch 4 with $\omega_0 = 6500$ rad/s

The slope of this line, 274 kJ/m, equals the energy required to drive a shear band through one meter. It is reasonable to conjecture that this value depends upon the material of the tube, its inner and outer radii, the criterion used to define a shear band, and the loading conditions. Noting that the width of the band is 0.119 mm and the external work done between the time it initiates in the element just below the notch tip and propagates to the innermost surface of the tube is 704 J, the energy required to drive a shear band through the material equals 126.2 J/mm³.

3.2 Effect of notch depth

Keeping the torsional loading pulse of 110 μ s total duration fixed, we varied the notch size by assigning values of 0.142, 0.221, 0.3, 0.379 and 0.458 mm to the depth, d , of the notch (cf. Fig. 1b); these notches are identified as 1, 2, 3, 4 and 5 respectively. The results presented in this section are for a maximum applied angular speed of 6500 rad/s. Figure 10a illustrates for notch 5 the distribution of different stress components on a radial line through the notch tip at time $t = 10$ μ s, when the deformations of the tube are expected to be elastic; it is evident that $\sigma_{z\theta}$ grows rapidly near the notch tip (z -axis is along the tube's axis) and all of the remaining stress components are at least an order of magnitude smaller. A closer look at their values reveals that σ_{rr} , σ_{zz} and $\sigma_{\theta\theta}$ remain essentially zero through the thickness of the tube, and σ_{zr} and $\sigma_{r\theta}$ while remaining small do exhibit a singular behavior. Extrapolating $\sigma_{z\theta}$ to the notch tip, and also evaluating it from

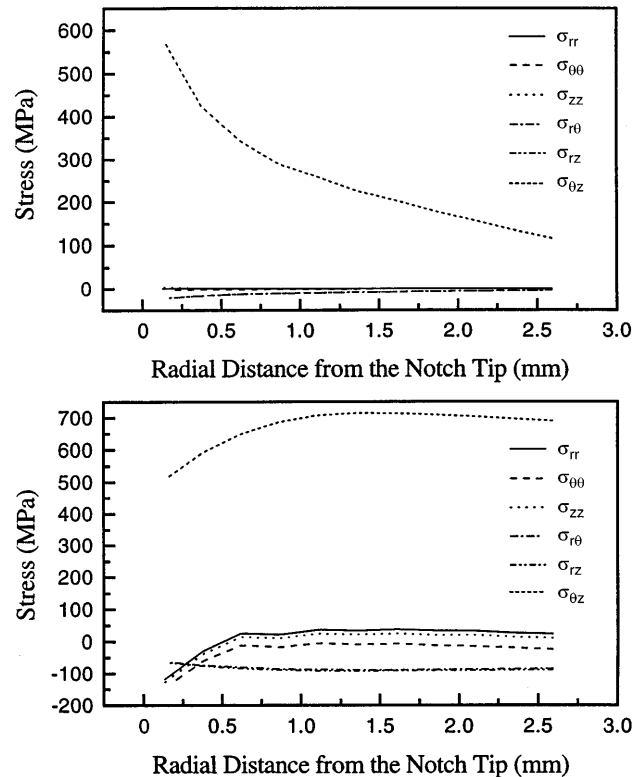


Fig. 10a,b. Stress distribution on a radial line for notch 5 with $\omega_0 = 6500$ rad/s at a $t = 10$ μ s, and b $t = 40$ μ s

Tr/J_e , where T is the torque, $J_e = \pi(r_o^4 - r_i^4)/2$, r_o and r_i being the outer and inner radii of the tube, and r is the radial distance of a point from the tube's axis, we obtain a stress concentration factor of 1.64 which agrees well with that given in Fig. 10.2 of Dowling's book (1993). A plot of $\sigma_{z\theta}$ vs. $1/\sqrt{s}$ where s is the radial distance from the notch tip gives a stress-intensity factor of $6.61 \text{ MPa } \sqrt{m}$. In Fig. 10b we have plotted the distribution of stress components on a radial line at $t = 40 \mu\text{s}$ when a part of the cross-section of the tube passing through the notch-tip has deformed plastically. Because of the softening of the material near the notch tip, caused by heating due to plastic deformation, $\sigma_{z\theta}$ near the notch tip is lower than that at other points on the radial line; the variation of $\sigma_{\theta\theta}$, σ_{zz} and σ_{rr} vs. s exhibits a singular behavior and their maximum magnitudes at the notch tip equal approximately one-fourth the magnitude of $\sigma_{z\theta}$ there. As expected, the stress distribution on a radial line is quite different when the material is undergoing plastic deformations as compared to that when it is deforming elastically. The stress state at points ahead of the shear band is triaxial.

Figure 11 depicts the dependence of the time of initiation of a shear band in an element just below the notch-tip upon the defect size defined as the notch depth, d , divided by the tube thickness at a cross-section away from the notch. Batra et al. (1996) used DYNA3D to study torsional deformations of a thin-walled tube whose thickness varied sinusoidally with the minimum thickness occurring at the midsection. They found that the average critical strain (or the time) at which a shear band initiated, as indicated by the sharp drop in the torque required to deform the tube, varied exponentially with the defect parameter $\epsilon = (1 - \text{minimum tube thickness}/\text{maximum-tube thickness})$. The slope of the average critical strain vs. $\log \epsilon$ curve was found to be independent of the nominal strain. These results are in qualitative agreement with the test results of Chi (1990), Murphy (1990), and Deltort

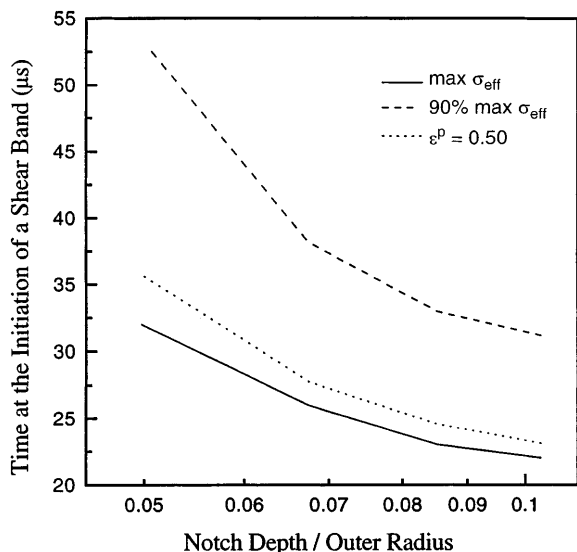


Fig. 11. Dependence of the time of initiation of a shear band upon the defect size as computed by three different criteria, for the case of $\omega_0 = 6500 \text{ rad/s}$

(1994), and analytical results of Molinari and Clifton (1987) and Wright (1994). For the thick-walled tube studied here, the curve representing the time of initiation of a shear band vs. \log (defect size) is not a straight line. This could either be due to an improper definition of the defect size, or different defect shape and/or the triaxiality of the stress-state near the notch tip; it does not depend upon the criterion used for the initiation of a shear band. We note that the analytical studies of Molinari and Clifton (1987) and Wright (1994) are for a simple shearing problem which is a good model for torsional deformations of a thin-walled tube.

In Fig. 12 we have plotted the time history of the torque required to deform the tube for each of the five notches. For notch 1 the torque continues to increase until $t = 90 \mu\text{s}$ when the prescribed angular speed begins to decrease, and no shear band initiates. The time when the torque starts to drop sharply decreases with an increase in the notch depth and for notch 5 the torque drops when the prescribed angular speed has reached its steady value of 6500 rad/s . For notch 2 a sharp drop in the torque commences at $t \approx 62 \mu\text{s}$ but a shear band initiates in an element below the notch tip at $t = 34, 36$ or $53 \mu\text{s}$ according to criteria (i), (ii) and (iii) of Section 3.1. A similar observation can be made for the other three notches. Thus the instant of the sharp drop in the torque required to deform the tube need not coincide with the time when a shear band first initiates at a point in the tube. Figure 13 illustrates, for notches 2 through 5, the external work done required to drive a shear band defined as the boundary of the region with an effective plastic strain of at least 0.5. We note that a part of the external work done is required to change the kinetic energy of the body. However, once a shear band has developed, the kinetic energy of the tube deformed by prescribing the angular speed at its end faces remains constant as long as the prescribed angular speed is uniform. During the time interval when the shear band propagates from $s = 1.0 \text{ mm}$ to $s = 2.5 \text{ mm}$, the slopes of the curves for notches 3, 4 and 5 equal 316, 274 and

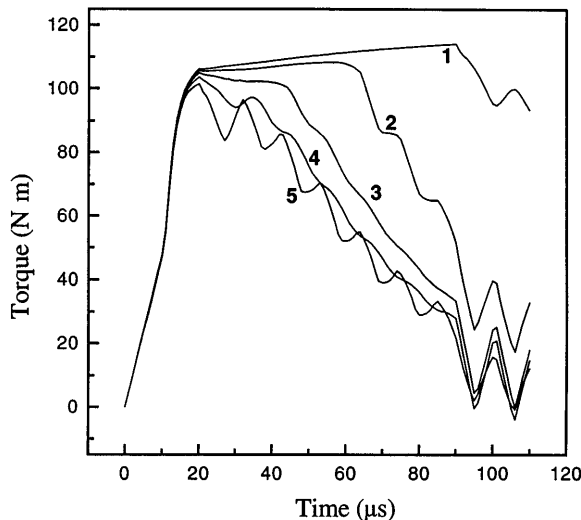


Fig. 12. Time history of the torque required to deform the tube for five different notches with $\omega_0 = 6500 \text{ rad/s}$

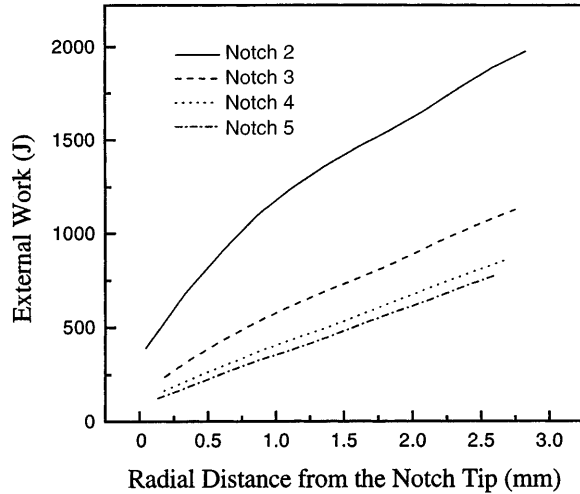


Fig. 13. External work done vs. the radial distance through which a shear band (a contour of effective plastic strain of 0.5) has propagated for notches 2, 3, 4 and 5 with $\omega_0 = 6500$ rad/s

260 kJ/m respectively; they give the energy required to drive a shear band through a unit distance.

The variation of the band speed with the radial distance from the notch tip for notches 2, 3, 4 and 5 is plotted in Fig. 14; the band is taken to initiate at a point when the effective plastic strain there equals 0.5. Except for the initial period during which the band propagates away from the notch tip, the band speed can be considered as essentially uniform, independent of the notch depth, and equals about 90 m/s. Thus the defect size influences the initial speed of a shear band but has very little effect upon its speed once it has propagated away from the defect.

3.3

Effect of prior axial loading

For the 4340 steel thick-walled tube with notch 5 at its center, we consider the loading history shown in Fig. 15. That is, the tube is first loaded by an axial compressive

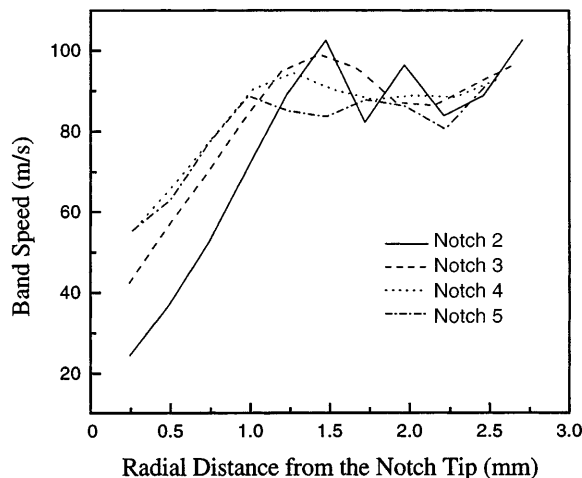


Fig. 14. Band speed vs. the radial distance through which a shear band (a contour of effective plastic strain of 0.5) has propagated for notches 2, 3, 4 and 5 with $\omega_0 = 6500$ rad/s

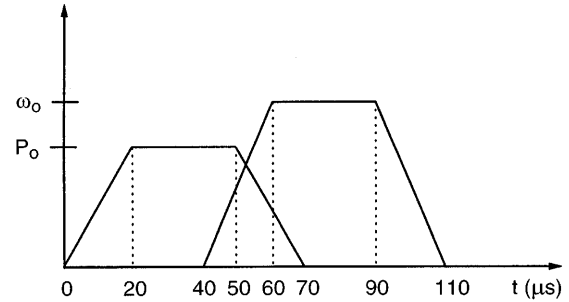


Fig. 15. Loading history for combined axial and torsional loading

pressure which increases from zero to the final value P_0 in 20 μs , is kept steady for 30 μs and then decreases to zero in 20 μs . Before the pressure begins to decrease at $t = 50$ μs , one end of the tube is held fixed and the other twisted by a prescribed angular speed that increases linearly from zero at $t = 40$ μs to 6500 rad/s at $t = 60$ μs , is held there till $t = 90$ μs and then decreases linearly to zero at $t = 110$ μs . Three steady values, 100, 500 and 1000 MPa, of the applied axial pressure are considered. We have also investigated two cases in which the axial traction is maintained at 500 MPa or -500 MPa, for $t \geq 20$ μs . Recalling that the quasistatic yield stress of the material at room temperature equals 792 MPa, the axial traction of 1000 MPa will deform the tube plastically prior to the application of the torsional loading. Because of stress concentration near the notch root, the axial traction of 500 MPa will also plastically deform the element abutting the notch tip. The above-mentioned loading histories should simulate those experienced by the rod deformed in a split compression and torsion Hopkinson bar. Since the compression wave travels faster than the torsion wave, the tube will first be deformed in compression and then in torsion; the delay time between the arrival of the two waves at a tube face depends upon the length of the incident bar. The combined loading considered herein is not meant to simulate any specific experimental set-up. Furthermore, in our simulations, one end face of the tube is kept fixed and the other loaded; this is dictated by the way the stipulated combined loading can be easily applied in DYNA3D. Preventing points on the fixed end from moving laterally, and those on the loaded end from moving radially, will induce additional stresses there. This local effect should not influence, for moderate values of the axial load, deformations of the material neighboring the notch at the midsection of the tube.

Figures 16a, 16b and 16c exhibit, for different values of the axial load, the time history of the effective stress, the effective plastic strain and the temperature at the centroid of an element just below the notch tip; we have also included results for the case when the pure torsional loading begins at $t = 40$ μs , and there is no axial load applied. We first discuss results for axial loads of finite duration. Because of the stress concentration at the notch tip, for $P_0 = 500$ MPa, the effective stress there exceeds the quasistatic yield stress of the material. However, since the axial load begins to decrease 10 μs after the torsional load is applied, by the time the prescribed angular speed

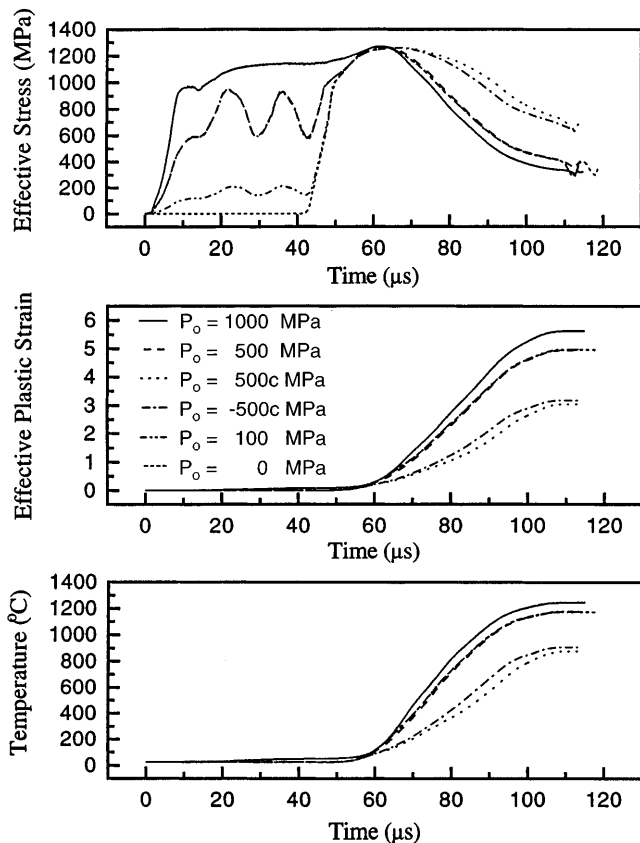


Fig. 16a-c. Time history of a the effective stress, b the effective plastic strain and c the temperature at the centroid of the element below the notch tip for notch 5 with combined axial and torsional loading

reaches its steady value the axial stress everywhere is below the yield stress of the material. Since $P_0 < A$, not much plastic strain is accumulated prior to the application of the torsional loading. However, for $P_0 = 1000$ MPa, the tube has been deformed plastically prior to being deformed in torsion. The plastic deformations caused by the torsional loading are significantly more than those induced by the axial compressive load. Except for $P_0 = 1000$ MPa, the effect of prior axial pressure is minimal on the plastic deformations of the element under the subsequent torsional loading. For $P_0 = 1000$ MPa, the prior plastic deformations of the element result in higher values of the effective plastic strain as compared to those affected by pure torsional loading.

For a constant pressure of ± 500 MPa, the effective stress drops gradually, and the effective plastic strain and the temperature rise slowly as compared to those for the other four cases; also the peak in the effective stress occurs later than that in the other four cases studied. Thus, the presence of axial stresses tends to delay the initiation of a shear band and the shear band grows less rapidly under combined axial and torsional loading as compared to that under the same pure torsional loading. Murphy (1990) has tested thin-walled steel tubes loaded first quasistatically in simple compression and then twisted dynamically. He found that an increase in the prior compressive load increased the nominal shear strain at which a shear band

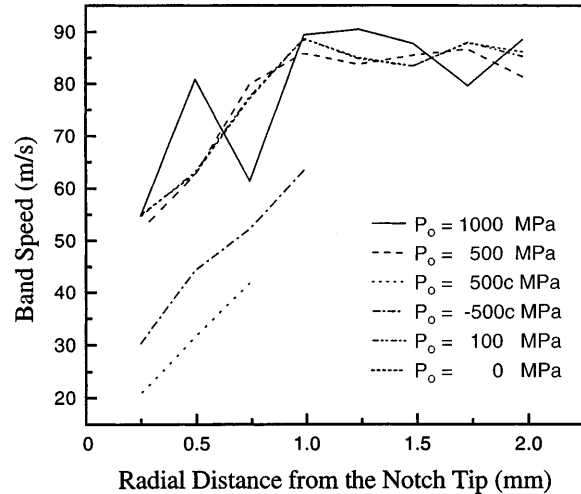


Fig. 17. Band speed in the radial direction for different axial loads vs. the radial distance through which a shear band (a contour of effective plastic strain of 0.5) has propagated for notch 5 with combined axial and torsional loading

initiated as indicated by the sharp drop in the shear stress or the torque required to deform the tube. Our computed result for the constant pressure of 500 MPa agrees qualitatively with Murphy's observations.

Figure 17 exhibits the variation of the band speed, defined as a contour of effective plastic strain of 0.5, as it propagates radially inwards through the thickness of the tube; it is evident that the prior axial loading does not significantly influence the speed of the band. However, when the axial traction is maintained, the band propagates radially through a much smaller distance and at a slower speed in comparison to that in the other four cases in which the axial load becomes zero by the time the applied angular speed attains its steady value. The band propagates a little further for tensile axial traction as compared to that for compressive loading of the same magnitude. We note that when the tube is loaded simultaneously in compression/tension and torsion, the maximum shear stress at a point need not occur on a surface perpendicular to the tube's axis. In order to compare results, we have determined in every case the speed of a shear band in the radial direction.

Figures 18a and 18b depict the time history of the effective stress and the effective plastic strain at the eleven elements on a radial line through the notch tip for the combined loading case with a constant tensile axial traction of $P_0 = 500$ MPa. Figure 18a shows that before the torsional load begins to drop at $90 \mu\text{s}$, the effective stress drops to 90% of its maximum value in only one element below the notch tip. It is evident from Fig. 18b that a contour of effective plastic strain of 0.5 propagates to five elements through the thickness during the first $90 \mu\text{s}$. This provides us with an example where the two definitions of the initiation of a shear band yield totally different answers for the distance through which a band propagates.

We note that the work done by the applied axial traction is essentially negligible as compared to that done by the torque; for example, the total work done by the constant

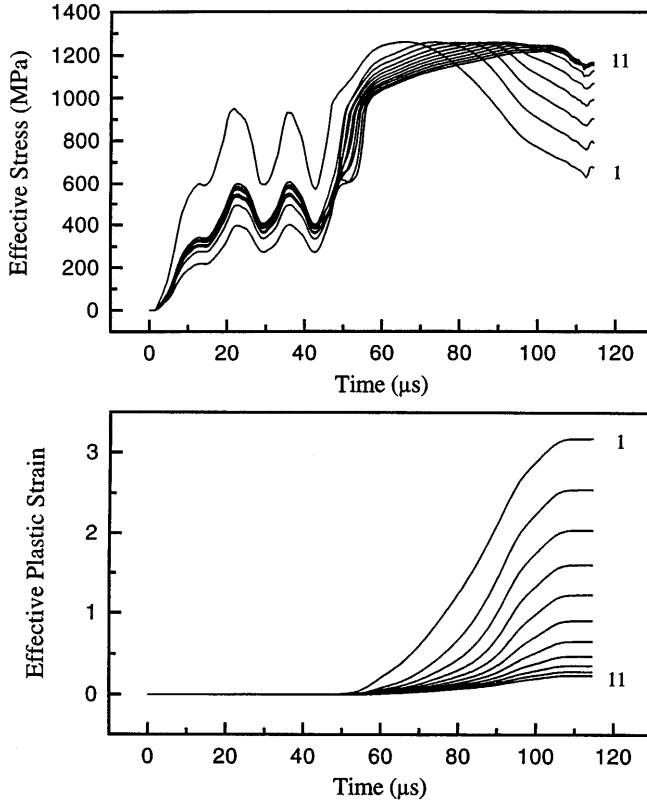


Fig. 18a,b. Time history a the effective stress and b the effective plastic strain at the centroids of eleven elements on a radial line through the notch tip for notch 5 for the case of combined tensile axial and torsional loading with $P_0 = 500$ MPa

axial pressure of 500 MPa during the load duration of $110 \mu\text{s}$ is only 3 J whereas that done by the torque is 1920 J. The results plotted in Fig. 19 clearly indicate that significantly more energy is required to drive a shear band for the case of combined loading as compared to that for pure torsional loading.

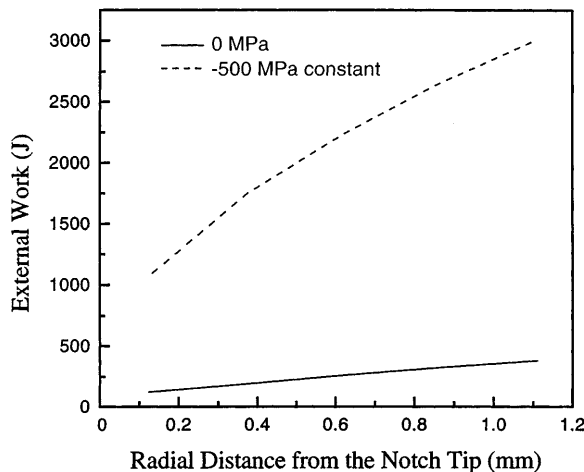


Fig. 19. External work done vs. the radial distance through which a shear band has propagated for notch 5 for the cases of pure torsional loading, and constant tensile axial loading combined with torsional loading

3.4

Torsion of a CR-300 steel tube

Zhou et al. (1996) have recently reported observed and computed shear band speeds in impact loaded prenotched CR-300 steel plates. Depending upon the impact speed, the observed average shear band speed varied from 50 m/s to 1000 m/s, and the corresponding computed average shear band speed ranged between 70 m/s and 1200 m/s. The failure mode in the impact loaded prenotched plate is close to Mode II and that in the torsional loading of a thick-walled tube is more like Mode III. A major difference between our and their numerical simulations is in the thermal softening function used in the constitutive relation (9)₂; thus we replace it by

$$\sigma_y = \max\left\{ (A + B(e^p)^n)(1 + C \ln(\dot{\epsilon}^p/\dot{\epsilon}_0)) [1 - \delta(\exp((T - T_0)/\kappa) - 1)], 0 \right\} \quad (16)$$

where T_0 equals the room temperature. Values of material parameters $A, B, n, C, \dot{\epsilon}_0, \delta$, and κ obtained by fitting curves to their data and of other material parameters used in the results reported herein are given below; geometric parameters were assigned values given in (13).

$$\begin{aligned} \rho_0 &= 7,830 \text{ kg/m}^3, & \mu &= 76.9 \text{ GPa}, & K &= 164.7 \text{ GPa}, \\ \delta &= 0.8 & A &= 2,000 \text{ MPa}, & B &= 94.5 \text{ MPa}, & n &= 0.2, \\ C &= 0.0165, & \theta_0 &= 293 \text{ K}, & \dot{\epsilon}_0 &= 1.3 \times 10^{-3}/\text{s}, \\ c &= 448 \text{ J/kg}^\circ\text{C}, & \kappa &= 500 \text{ K} \end{aligned} \quad (17)$$

For

$$T > \kappa \ln(1 + \delta) + T_0 \quad (18)$$

the expression on the right hand side of (16) will be negative; thus $\sigma_y = 0$. For the values of the material parameters given in (17), $\sigma_y = 0$ for $T = 698$ K which implies that the melting temperature of the material has been taken to be too low. We also investigate the problem for $\kappa = 800$ K which corresponds to a melting temperature of the material of 941 K. Zhou et al. (1996) also assumed that a material point failed if e^p there equaled 0.40 and it subsequently behaved as a nonlinear viscous fluid. Here we do not adopt this failure criterion and assume that a material point behaves as a perfect fluid once $\sigma_y = 0$ there. Because of the Lagrangian formulation used in DYNA3D, a fluid element will undergo intense deformations in essentially no time and the finite element mesh will become severely distorted resulting in an unacceptable size of the time step. The thermal softening function of Eq. (16) was incorporated into the material subroutine in DYNA3D.

We investigate the torsional deformations of the CR-300 steel thick-walled tube under the loading conditions of Sect. 3.1, with $\omega_0 = 6500$ rad/s and a load duration of $70 \mu\text{s}$. Figure 20 exhibits the time history of the effective stress, effective plastic strain and temperature at the centroids of two elements – one element just below the notch tip and the other adjoining the inner surface of the thick-walled tube with notch 5 at its midsection. For $\kappa = 500$ K, a shear band initiates, according to criterion (iii) of Sect. 3.2, in the element below the notch tip at $t = 23.5 \mu\text{s}$ and propagates to the inner surface of the tube in $2.8 \mu\text{s}$. The stress drop in each element is quite rapid and resembles

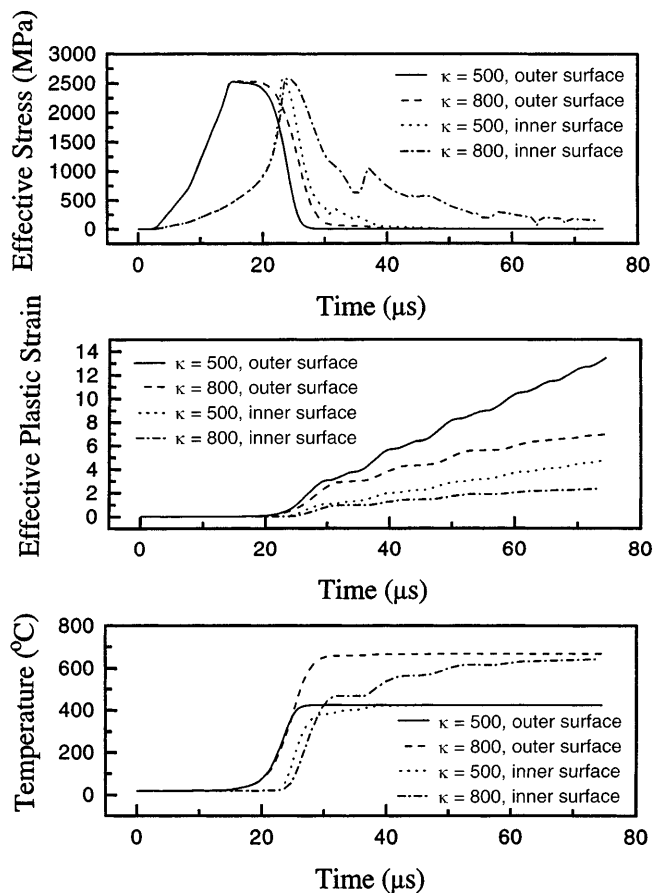


Fig. 20a-c. Time history of a the effective stress, b the effective plastic strain and c the temperature at two elements – one just below the notch tip and the other adjoining the inner surface of a CR-300 steel thick-walled tube with notch 5 deformed in torsion

that observed by Marchand and Duffy (1988) in a thin-walled tube. For $\kappa = 800$ K, the shear band initiates at $t = 24.2 \mu\text{s}$ and the stress drop is less catastrophic than that for $\kappa = 500$ K. Thus, the value of κ in the thermal softening function slightly influences when a shear band initiates in an element, but strongly affects the subsequent rate of drop of the effective stress there. The time history plots of the temperature verify the assertion that once $\sigma_y = 0$ in an element, its temperature does not change. This is because there is no more plastic working for that element and the deformations are presumed to be locally adiabatic.

The variation of the band speed with the radial distance from the notch tip is shown in Fig. 21, for two different initiation criteria; as expected the results depend upon the definition of the initiations of a shear band. If a shear band initiates at a material point when the effective plastic strain there equals 0.50, then the band speed varies from 750 m/s (450 m/s) to 1000 m/s (700 m/s) for $\kappa = 500$ K (800 K). However, if a shear band is taken to initiate at a point when the effective stress there has dropped to 90% of its maximum value, then the band speed increases from 300 m/s (300 m/s) to 1500 m/s (900 m/s) for $\kappa = 500$ K (800 K) as its propagates from the notch tip to the inner surface. These values are in the same range as those observed by Zhou et al., but the maximum temperatures

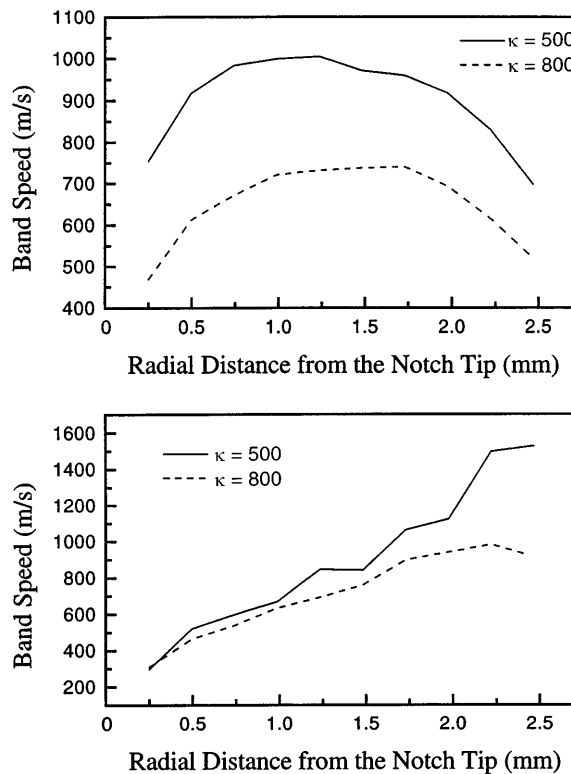


Fig. 21a,b. Band speed vs. the radial distance from the notch tip of a shear band in a CR-300 steel thick-walled tube with notch 5 deformed in torsion, as computed by the criteria a of effective plastic strain of 0.50, and b a drop to 90% of the maximum effective stress

computed herein are lower than those reported by them. Their plots of the time history of the speed of a shear band lend credence to the definition of a shear band as a contour of effective plastic strain of say 0.5. However, Marchand and Duffy (1988) suggest that a shear band initiates when the shear stress drops catastrophically.

Figure 22 depicts the external work done as a function of the radial distance, s , through which a shear band (a contour

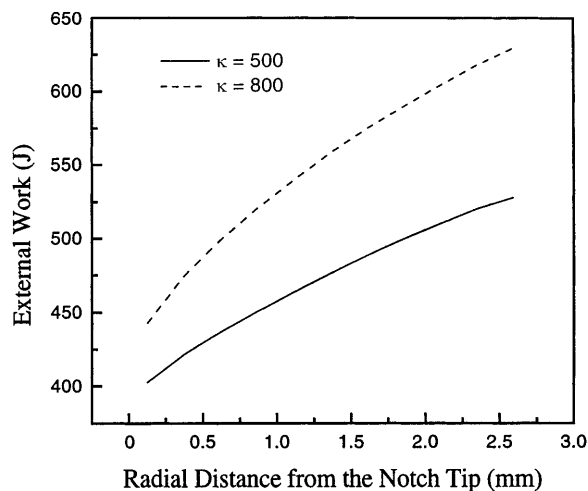


Fig. 22. External work done vs. the radial distance through which a shear band (a contour of effective plastic strain of 0.5) has propagated for torsional deformations of the CR-300 steel thick-walled tube with notch 5

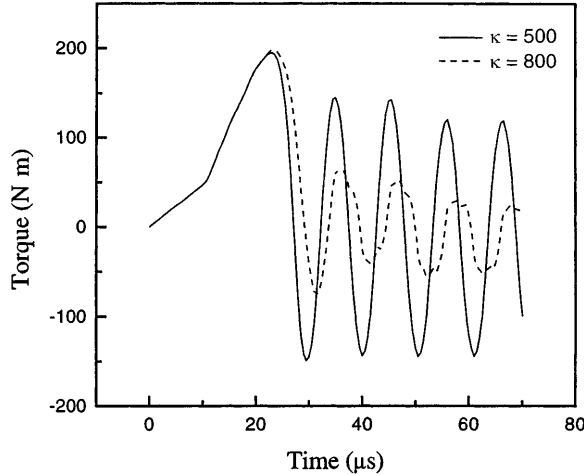


Fig. 23. Time history of the torque required to deform the CR-300 steel thick-walled tube with notch 5

of effective plastic strain of 0.5) has propagated. As expected, less work is needed to drive the shear band for $\kappa = 500$ K as compared to that for $\kappa = 800$ K. The slopes of these curves for $1.0 \text{ mm} \leq s \leq 2.6 \text{ mm}$ are 45.2 J/mm and 60.7 J/mm for $\kappa = 500$ K and $\kappa = 800$ K respectively; these equal the energy required to drive a shear band radially inwards through 1 mm on the cross-section through the notch tip. Since the shear band width equals 0.119 mm, the average energy required to shear band the material equals 23.4 and 34.9 J/mm^3 for the two values of κ .

We have plotted in Fig. 23 the time history of the torque required to deform the tube. Once a shear band has developed at the cross-section through the notch tip, the effective stress there drops sharply and an elastic unloading wave which emanates results in the oscillations in the applied torque. The amplitude of this unloading wave is related to the drop in the effective stress and is less for the larger value of κ because of decreased thermal softening of the material. The period of these oscillations approximately equals the time taken for a shear wave to traverse through twice the length of the tube. We recall that one end of the tube is kept stationary and the other is twisted with a prescribed angular speed. The negative torque means that it acts in a direction opposite to that of twisting. Of course this is not possible for linear elastic materials, but here an elasto-thermo-visco-plastic material is undergoing large deformations. Batra and Kim (1990) seem to be the first to compute the elastic unloading wave in their study of the development of shear bands in a steel block undergoing simple shearing deformations; their computed shear stress on the shearing plane opposed the shearing direction. The oscillations in the torque will not occur for large values of κ since the stress will drop gradually within the shear band. The amplitude of the oscillations decreases because of the energy dissipated due to plastic deformations of the tube.

The distribution at $t = 10.5 \mu\text{s}$ and $30.5 \mu\text{s}$ of different components of stress on a radial line through the notch tip for $\kappa = 800$ K is exhibited in Figs. 24a and 24b respectively. At $t = 10.5 \mu\text{s}$, the deformations of the tube are essentially elastic and at $t = 30.5 \mu\text{s}$ a shear band, as in-

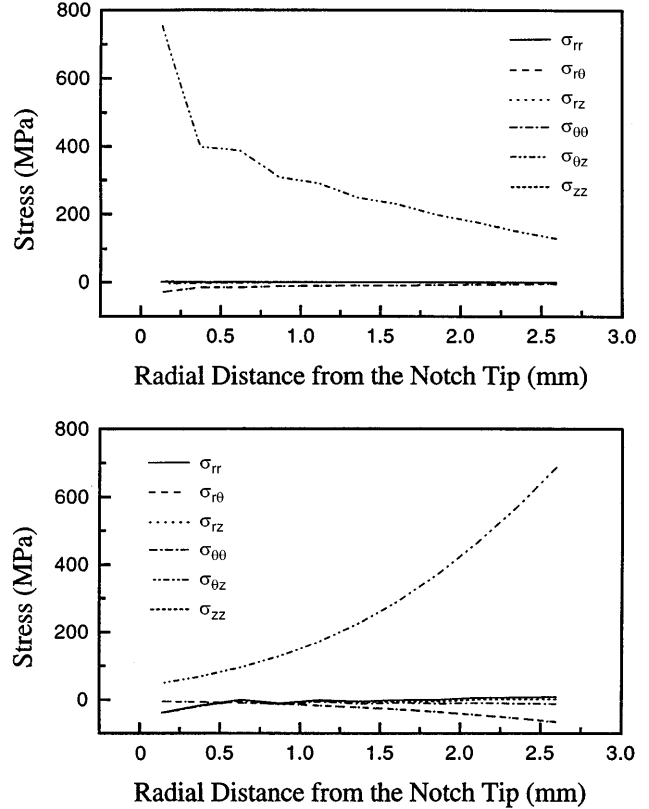


Fig. 24a,b. Distribution of the different components of stress on a radial line through the notch tip for torsional deformations of the CR-300 steel thick-walled tube with notch 5 for $\kappa = 800$ K, at a $t = 10.5 \mu\text{s}$ and b $t = 30.5 \mu\text{s}$

indicated by the accumulation of plastic strain, has initiated and propagated to the inner surface of the tube. Whereas at $t = 10.5 \mu\text{s}$, $\sigma_{z\theta}$ (z -axis is along the tube's axis) is maximum at the notch tip, it is minimum there at $t = 30.5 \mu\text{s}$; this is due to the softening of the material caused by heating from the intense plastic deformations.

4 Conclusions

We have studied dynamic thermomechanical finite deformations of a thick-walled 4340 steel tube subjected to torsion, and combined torsional and axial pressure loading. The tube material is modeled as elastic-thermo-viscoplastic with the flow stress depending upon the effective plastic strain, effective plastic strain-rate and temperature. The tube has a V-notch at the midsection which acts as a stress concentrator. The loading pulse is of finite duration with a rise and fall-off time of $20 \mu\text{s}$ each and stays steady for some time in between; thus a finite amount of energy is input into the body.

Under pure torsional loading a shear band, identified by a drop in the effective stress to 90% of its peak value or the effective plastic strain reaching a preassigned value, initiates first in an element below the notch tip and propagates radially inwards. Its speed of propagation varies from 50 m/s at the time of initiation to a maximum of about 100 m/s as it reaches the innermost surface of the tube. The temperature rise at the initiation of a shear band is

nearly 130°C but the temperature reaches approximately 95% of the melting temperature of the material 70 μ s later. When the loaded end face of the tube has been brought to rest at $t = 110 \mu$ s, sharp gradients in the temperature and effective plastic strain develop through the shear-banded region. The energy required to shear band the material equals 126.2 J/mm³.

During elastic deformations of the tube under pure torsional loading, only the $\sigma_{z\theta}$ component of the Cauchy stress exhibits noticeable stress concentration at the notch tip and other components of the stress tensor have negligible values everywhere. However, when the cross-section through the notch tip has deformed plastically, $\sigma_{z\theta}$ at the notch tip has the lowest value. Other components, $\sigma_{\theta\theta}$, σ_{zz} and σ_{rr} take on maximum values at the notch tip which equal approximately one-fourth of the maximum magnitude of $\sigma_{z\theta}$. The time of initiation of a shear band decreases exponentially with the depth of the notch; however, the notch depth influences only the initial speed of a shear band. After the band has propagated radially inwards, its speed is essentially independent of the notch depth and equals about 90 m/s.

For combined torsional and axial loading, the shear band initiates later and propagates slower than that for pure torsional loading. Also, for the case of combined loading, different definitions of the initiation of a shear band give contradictory results in the sense that according to one criterion a shear band initiates at a point because the effective plastic strain there reaches the preassigned value of 0.5, but according to another criterion it does not initiate because the effective stress there does not drop to 90% of its peak value for that material point.

For torsional loading of a CR-300 steel thick-walled tube with the thermal softening modeled by the relation proposed by Zhou et al. (1996), the computed maximum shear band speed of 1000 m/s agrees with that observed by them in their impact experiments on prenotched plates. Because of the presumed enhanced thermal softening, the effective stress drops catastrophically in the shear banded region, and an elastic unloading wave emanates from there. It results in oscillations in the torque required to deform the tube, and during some time intervals, the torque acts in a direction opposite to that of the prescribed angular speed. The energy required to drive the shear band radially inwards on the cross-section through the notch tip strongly depends upon the parameters characterizing the thermal softening of the material. For $\kappa = 500$ K in Eq. (16), the energy required to shear band the material equals 23.4 J/mm³.

References

- Anand, L.; Kim, K. H.; Shawki, T. G. (1987): Onset of shear localization in viscoplastic solids. *J Mech Phys Solids* 35, 381–399
- Armstrong, R.; Batra, R. C.; Meyers, M. A.; Wright, T. W. (Eds.) (1994): Special issue on shear instabilities and viscoplasticity theories. *Mech Mater* 17, 83–327
- Batra, R. C.; Adulla, C. (1995): Effect of prior quasistatic loading on the initiation and growth of dynamic adiabatic shear bands. *Arch Mechs* 47, 485–498
- Batra, R. C.; Jin, X. S. (1994): Analysis of dynamic shear bands in porous thermally softening viscoplastic materials. *Arch Mech* 41, 13–36
- Batra, R. C.; Kim, C. H. (1990): Adiabatic shear banding in elastic-viscoplastic nonpolar and dipolar materials. *Int J Plasticity* 6, 127–141
- Batra, R. C.; Kim, C. H. (1991): Effect of thermal conductivity on the initiation, growth, and band width of adiabatic shear bands. *Int J Eng Sci* 29, 949–960
- Batra, R. C.; Kim, C. H. (1992): Analysis of shear bands in twelve materials. *Int J Plasticity* 8, 75–89
- Batra, R. C.; Ko, K. J. (1992): An adaptive mesh refinement technique for the analysis of shear bands in plane strain compression of a thermoviscoplastic block. *Comp Mech* 10, 369–379
- Batra, R. C.; Zbib, H. M. (Eds.) (1994): *Material instabilities: theory and applications*. ASME Press, New York
- Batra, R. C.; Zhang, X. (1994): On the propagation of a shear band in a steel tube. *J Eng Mat Tech* 116, 155–161
- Batra, R. C.; Adulla, C.; Wright, T. W. (1996): Effect of defect shape and size on the initiation of adiabatic shear bands. *Acta Mech* 116, 239–243
- Chi, Y. C. (1990): Measurement of the local strain and temperature during the formation of adiabatic shear bands in steel. Ph.D. Thesis, Brown University
- Clifton, R. J. (1980): Adiabatic shear. In: Herrman, W. et al. (eds.), *material response to ultrahigh loading rates* U.S. NRC Material Advisory Board Report NMAB-356
- Deltort, B. (1994): Experimental and numerical aspects of adiabatic shear in a 4340 steel. *J Physique Colloque C8*, 4, 447–452
- Dowling, N. E. (1993): *Mechanical Behavior of Materials: engineering methods for deformation, fracture and fatigue*. Prentice-Hall, Englewood Cliffs, NJ
- Farren, W. S.; Taylor, G. I. (1925): The heat developed during plastic extrusion of metal. *Proc R Soc A207*, 422–426
- Johnson, G. R.; Cook, W. H. (1983): A constitutive model and data for metals subjected to large strains, high strain rates and high temperatures. *Proc. 7th Int. Symp. Ballistics*, The Hague, The Netherlands, 541–548
- Klepackzko, J. R.; Lipinski, P.; Molinari, A. (1987): An analysis of the thermoplastic catastrophic shear in some metals. In: Chim, C. Y.; Kunze, H.-D.; Meyer, L. W. (eds.) *Impact Loading and Dynamic Behavior of Materials*, Informationsgesellschaft Verlag, Bremen, 695–704
- Marchand, A.; Duffy, J. (1988): An experimental study of the formation process of adiabatic shear bands in a structural steel. *J Mech Phys Solids* 36, 251–283
- Molinari, A.; Clifton, R. J. (1987): Analytical characterization of shear localization in thermoviscoplastic materials. *J Appl Mech* 54, 806–812
- Murphy, B. P. (1990): Shear band formation in a structural steel under a combined state of stress. M.S. Thesis, Brown University
- Peng, Z.; Batra, R. C. (1995): Propagation of shear bands in thick-walled RHA steel tubes. In: Atluri, S. N.; Yagawa, Y.; Cruse, T. A. (eds.) *Comp Mechanics 95*, Springer-Verlag, 2034–2039
- Rajendran, A. M. (1992): High strain rate behavior of metals, ceramics and concrete. Report #WL-TR-92-4006, Wright Patterson Air Force Base
- Sulijoadikusumo, A. V.; Dillon Jr., O. W. (1979): Temperature distribution for steady axisymmetric extrusion with an application to Ti-6Al-4V, part 1. *J Therm Stress* 2, 97–112
- Tresca, H. (1878): On further application of the flow of solids. *Proc Inst Mech Eng* 30, 301–345
- Truesdell, C. A.; Noll, W. (1965): The nonlinear field theories of mechanics. In: Flügge, S. (ed) *Handbuch der Physik*, Vol. III/3, Springer-Verlag, Berlin
- Whirely, R. G.; Hallquist, J. P. (1991): *DYNA3D User's Manual*, a nonlinear, explicit, three-dimensional finite element code for solid and structural mechanics. User Manual, Lawrence Livermore National Laboratory Report, UCRL-MA-107254
- Wright, T. W. (1994): Toward a defect invariant basis for susceptibility to adiabatic shear bands. *Mech Mat* 17, 215–222

Wright, T. W.; Walter, J. W. (1987): On stress collapse in adiabatic shear bands. *J Mech Phys Solids* 35, 701–716
Zbib, H. M.; Shawki, T.; Batra, R. C. (Eds) (1992): Material instabilities. *Appl Mech Rev* 45:3, (Special Issue)

Zener, C.; Hollomon, J. H. (1944): Effect of strain rate on plastic flow of steel. *J Appl Phys* 14, 22–32
Zhou, M.; Rosakis, A. J.; Ravichandran, G. (1996): Dynamically propagating shear bands in impact-loaded prenotched plates II – numerical simulations. *J Mech Phys Solids* 44, 1007–1032